JTTEE5 8:73-78

Improving the Methodology for Coating Defects Detection

N. Llorca-Isern, M. Puig, and M. Español

(Submitted 20 July 1998; in revised form 21 September 1998)

A vacuum impregnation procedure for examining the microstructure of thermal spray coatings has been evaluated using a low-viscosity fluorescent resin. The use of confocal laser scanning microscopy for examining the microstructure allows three-dimensional image reconstruction of the sample. Relationships between defects (i.e., porosity or micro/macrocracking) and coating properties can be established more accurately with the proposed methodology because it enables quantitative analysis.

Keywords adhesion, characterization, cohesion, confocal microscopy, porosity, thermal spray coatings, three-dimensional reconstruction

1. Introduction

The microstructure of thermal spray coatings is very complex because of the many features that can be observed. From a "defect" point of view, general features that are found include: porosity (micro or macro), microcracks (thin and short or long), and/or macrocracks (thick and short or long), all of these being isolated or connected. Cracks can be localized inside the coating. The term" lack of coherency" is used when cracks run perpendicular to the spraying direction, the term "cohesive" cracking applies when they are parallel to the substrate and within the coating, and "adhesive" cracking means they are located at the coating/substrate interface. Coating properties are related to the quantity of defects and the quality in terms of connectivity between them. Therefore, it is important to evaluate defects as precisely as possible. Different problems arise when the sample to be characterized is metallographically prepared. If specimen preparation is not carried out carefully, then the real number, size, and morphology of these defects can be altered. References 1 to 5 detail the prior work in the area of metallographic preparation.

It has been well established that the first step in metallographic specimen preparation of sprayed coatings is to impregnate the sample under vacuum with a resin (Ref 6). Using the benefits of this recommendation, fluorescent dye can be added to the resin (Ref 2), and thus the specimen can be observed under a fluorescent microscope. Moreover, using a low-viscosity resin with fluorescent dye under a high vacuum, the impregnation will be more effective and, if the observation is then carried out with a confocal laser scanning microscope (CLSM), three-dimensional information can be obtained.

This article details an improvement of the method to study defects that has little influence on the preparation step. Moreover, use of the CLSM gathers information at different vertical optical sections of the specimen, and their recombination results in a three-dimensional image of the coating and thus determination of the relationships between defects (Ref 7).

N. Llorca-Isern, M. Puig, and **M. Español,** Dept. E.Q.-Metallurgia, Fac. Quimica, Universitat de Barcelona, Marti-Franques 1, E-08028 Barcelona, Spain. Contact e-mail: llorca@angel.qui.ub.es.

2. Experimental Method

2.1 Vacuum Impregnation

It is necessary to vacuum impregnate the specimen for maximum resin penetration into the pores and through the cracks. The first method used was to immerse the specimen in a premixed fluorescent low-viscosity polyester resin curing at ambient temperature and then apply the vacuum. Using a rotary pump, 10^{-2} Pa is reached. Under these conditions, the induction time for resin hardening is very low and the penetration of the resin into the sample is not satisfactory, especially if the thickness of interconnected defects reaching the surface is small. Three possibilities have been studied to improve this procedure:

- The choice of a lower viscosity epoxy resin
- The improvement in vacuum conditions by using a diffusion pump baked with a rotary (10^{-5} Pa) pump
- The simultaneous but independent evacuation of the sample and the resin as suggested by Karthikeyan et al. (Ref 6)

Polyester (Fontanals S.A., Cornella, Spain) and epoxy (Fluka, Switzerland, and Sigma, St. Louis, MO, USA) resins were selected for their low viscosity as well as for their different activation time. The former could be used at ambient temperature, its viscosity being 3.0 Pa · s, while the latter was a modified Spurr epoxy resin (Ref 8) chosen for its higher curing temperature (60 °C) and its low viscosity of 0.8 Pa · s. This difference in curing temperature, together with the fluidity of the resin, was shown to be critical when there was a need for efficient evacuation and impregnation of the sample. The only disadvantage is the curing time; for this resin 48 h are needed for complete hardening. Epodye (Struers, Westlake, OH, USA) was the selected fluorescent compound because it exhibited good mixing capacity with the resin.

Two procedures were performed for vacuum impregnation of the samples. The method of Karthikeyan et al. (Ref 6) consisted of controlled evacuation of the sample and resin independently, which were then mixed in the chamber. The other method consisted of combining the resin and sample prior to evacuation.

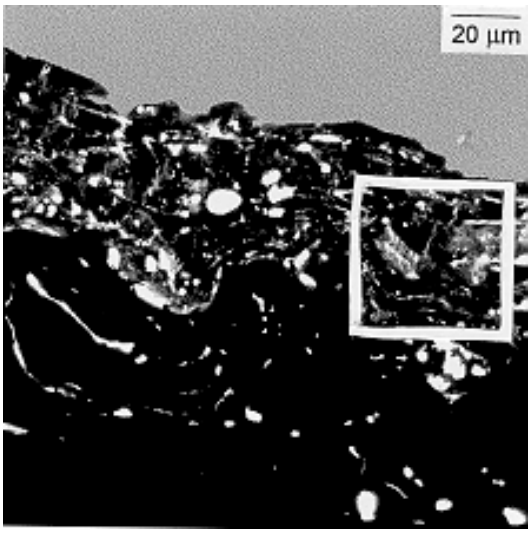

(a)

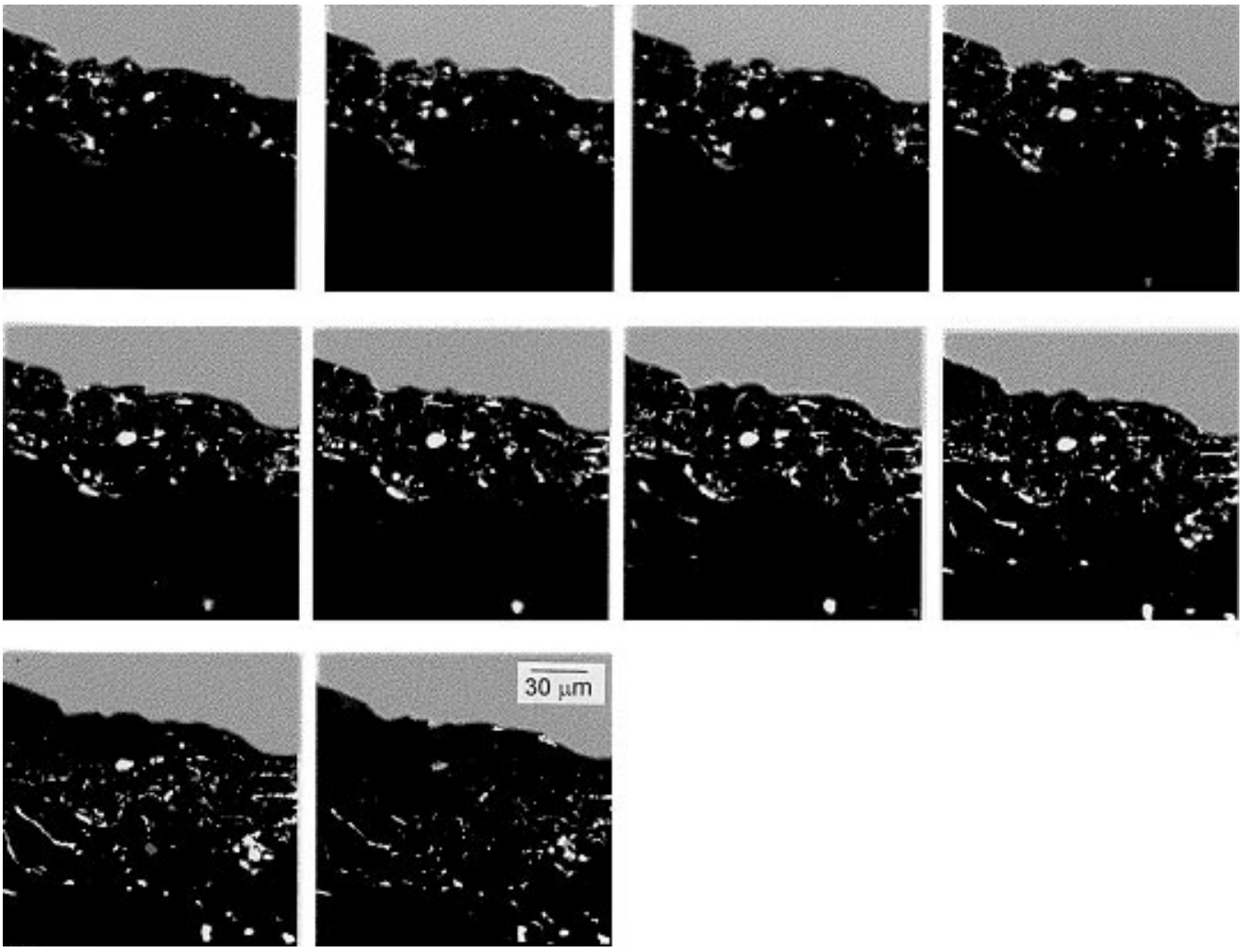

(b)

Fig. 1 (a) CLSM three-dimensional reconstruction of *x-y* optical sections corresponding to a volume of 160 by 160 by 10 μm^3. (b) CLSM series of 10 *x-y* optical sections. HVOF-thermal barrier coating cross sections. High-vacuum impregnation with fluorescent modified Spurr resin of premixed sample + resin procedure

Previous work (Ref 9) has indicated an influence of the vacuum level, and this was studied using rotary and diffusion pumps at pressure levels of 10^{-2} and 10^{-5} Pa, respectively.

2.2 Specimens

Different thermal sprayed samples have been tested: high-velocity oxygen fuel (HVOF) thermal barrier and air plasma sprayed (APS) and radio frequency (RF) inductive plasma ceramic coatings. They have been sprayed under different conditions to produce different levels of porosity and microcracks. The coating thickness varied from 120 to 650 μm.

2.3 Confocal Laser Scanning Microscope

Observations were carried out with an optical CLSM Leica TCS 4D (Leica Laser Technik GmbM, Heidelberg, Germany) equipped with an argon-krypton laser source (75 mW, 488 nm). The principle of this technique is to collect, by means of a pinhole (variable diameter diaphragm) situated in front of the detector, reflected, diffracted, and fluorescent rays coming from the focal plane of the objective lens. Any other part of the beam coming from other focal planes is limited and does not contribute to formation of the image. The pinhole scans the *x-y* surface of the sample. This microscope can visualize optical *z*-sections of the fluorescent resin paths through the specimen and build up a three-dimensional reconstructed image. The depth of the observed volume depends on the movement of the microscope stage along the *z*-direction. Three-dimensional images are obtained by "cutting optically" the sample with the laser penetration at selected Δz; each section being digitally stored and finally reconstructed. There is no need to mechanically section the sample, and therefore no mechanical deformation affects the measurements. One advantage of this microscope is improvement in the lateral resolution in comparison with standard fluorescent microscopes (objectives of 20, 40, and 63× with lateral resolutions of 0.5, 0.35, and 0.14 μm, respectively, were used in this work). As well, the microscope has a high-resolution *z*-stage (2.6, 1.3, and 0.24 μm for 20, 40, and 63× objectives, respectively), a single-channel detector unit for confocal reflection or fluorescence microscopy, and a continuous varying computer-controlled pinhole. The standard Leica CLSM software and three-dimensional Leica software were used to record and process the images in three dimensions.

3. Results and Discussion

3.1 Methodology

Figure 1(a) shows a reconstructed image of a thermal barrier coating (TBC) of fluorescent modified Spurr resin impregnated sample under a 10^{-5} Pa vacuum, following the premixed evacuation procedure. It corresponds to 10 *x-y* optical sections 1 μm apart of 150 by 150 by 10 μm^3 volume (Fig. 1b). The curing temperature of 60 °C allowed the vacuum penetration of the resin to be maintained longer because it remained fluid. As can be seen in the figure, the fluorescent resin is observed deep inside the coating and reaches to the substrate/bond-coat interface, revealing a large number of microcracks and porosity of different sizes.

Figure 2(a) shows a series of 9 *x-y* optical sections 1.12 μm apart corresponding to a scanned part of the sample (detail indicated in Fig. 1). The volume under observation is 41 by 41 by 10 μm^3. The maximum depth of the observed volume depends on the transmission of laser light through the sample. The resin possesses excellent optical conditions. Thus, if the pores and cracks (macro or micro) are connected and resin penetration occurs, an image of the spatial network can be produced by projecting together the *x-y* sections (Fig. 2b) (the volume under observation is 41 by 41 by 10 μm^3). Other methods for impregnation by metals or their salts may also be used (Ref 10, 11). The main practical disadvantage is that it is impossible to impregnate the sample in a one-step procedure, and, in the case described here, this precluded detection of details under a CLSM. It is worth noting that this is the only technique where a three-dimensional path can be visualized continuously without mechanical preparation.

Porosity or a modification of its size or shape due to metallographic preparation would not be visualized under the microscope because fluorescence would be absent in such cases. The series in Fig. 2(a) shows the evolution of the defects in the *z*-axis, a requirement for accurate quantitative analysis. The main advantage of this optical microscopy method is that areas from underneath the surface can be studied, providing additional information.

3.2 Thin Network Defects

When the coating contains very fine cracks, the separate evacuation of the sample and resin at high vacuum is more suitable. Examples are shown in Fig. 3 and 4, corresponding to the same APS sprayed partially stabilized zirconia (PSZ) on a different substrate and resulting in different microcrack sizes. The spraying conditions are: $36Ar/12H_2$ for plasma gas flow rate, arc current of 600 A, and a spray distance of 100 mm (Ref 12). As can be seen, the amount of impregnation is different as well as the fluorescence, thereby showing the density of defects. Figure 3(a) shows a general view of the sample, which has been impregnated from the free surface of the coating. The fluorescent particles can be seen at the coating/substrate interface. The volume under observation was 500 by 500 by 21 μm^3. Figure 3(b) is a detail of Fig. 3(a). It corresponds to the reconstruction of 7 *x-y* optical sections (61.4 by 61.4 by 6 μm^3) at the coating/substrate interface. Figure 4(a) is the reconstruction of 16 *x-y* optical sections (volume 500 by 500 by 16.5 μm^3) and reveals a lower density of defects. The impregnation has been limited due to the characteristics of the sprayed system (Ref 12). Figure 4(b) is a detail from the top part of the coating. The results agree with the expected response of the material.

One way to express the fissure density is by evaluating the fissure volume following the Cavalieri formula (Ref 13) where the volume of any object V_{obj} can be estimated from parallel sections separated by a known distance *d*, summing the areas of all sections ΣA_i and multiplying this by *d*:

$$V_{obj} = d \cdot \Sigma A_i$$

$$\% \text{ defect} = \frac{d \cdot \Sigma A_i}{V_T} = \frac{\Sigma A_i}{n \cdot A_{xy}}$$

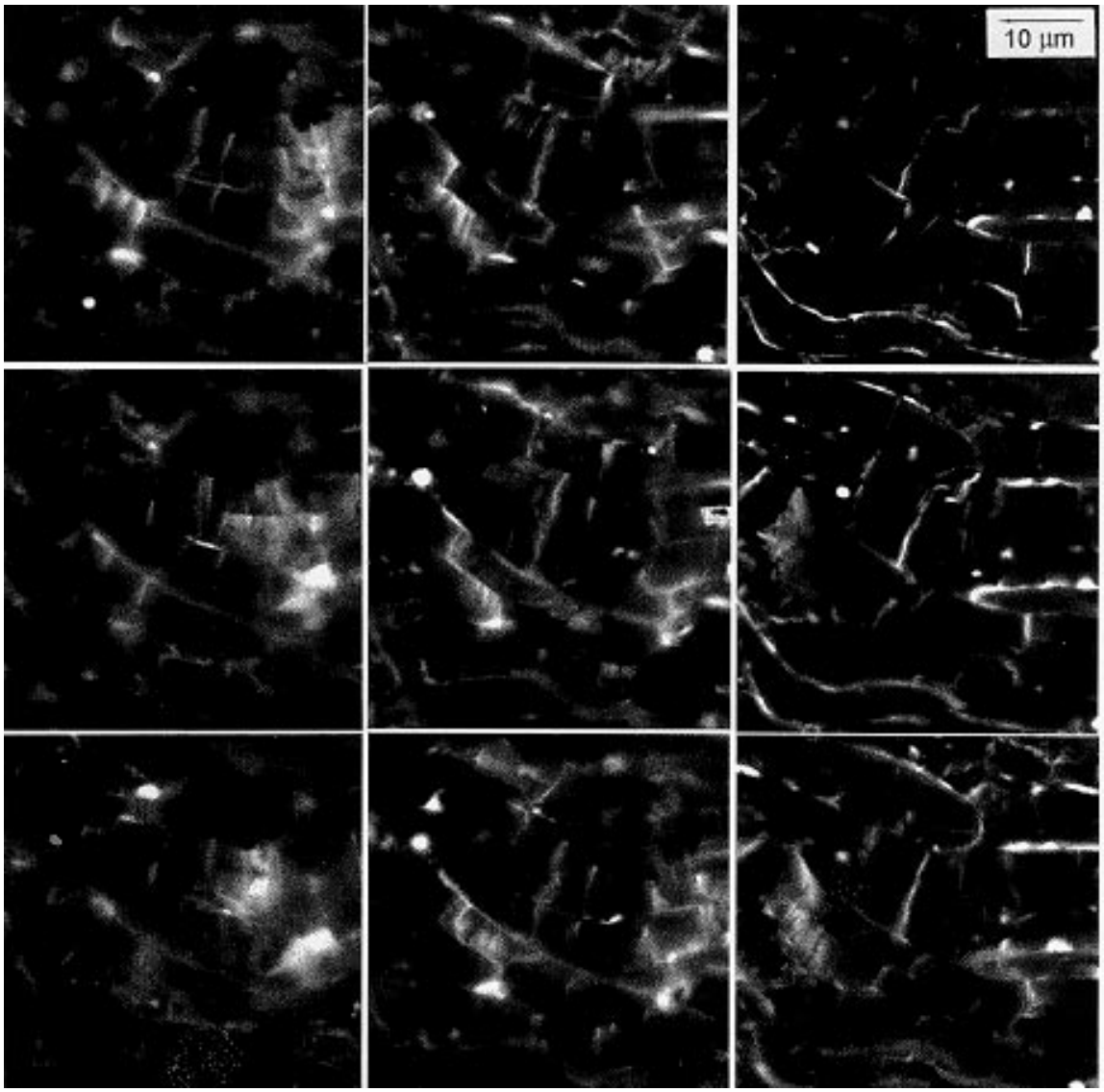

(a)

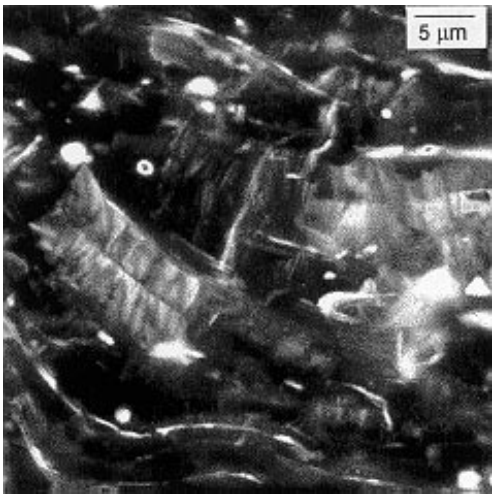

(b)

Fig. 2 (a) CLSM series of 9 *x-y* optical sections corresponding to a detail in Fig. 1. (b) CLSM three-dimensional reconstruction of Fig. 2(a). The volume under observation is 41 by 41 by 10 μm^3.

where $V_T = A_{xy} \cdot n \cdot d$, A_{xy} is the observed area, and n is the number of sections. The percentage of defects in the ceramic coating of the TBC sample (Fig. 2) using the above equation is $9 \pm 1\%$.

4. Conclusions

Coatings produced by thermal spraying contain defects requiring vacuum impregnation with low-viscosity epoxy resin.

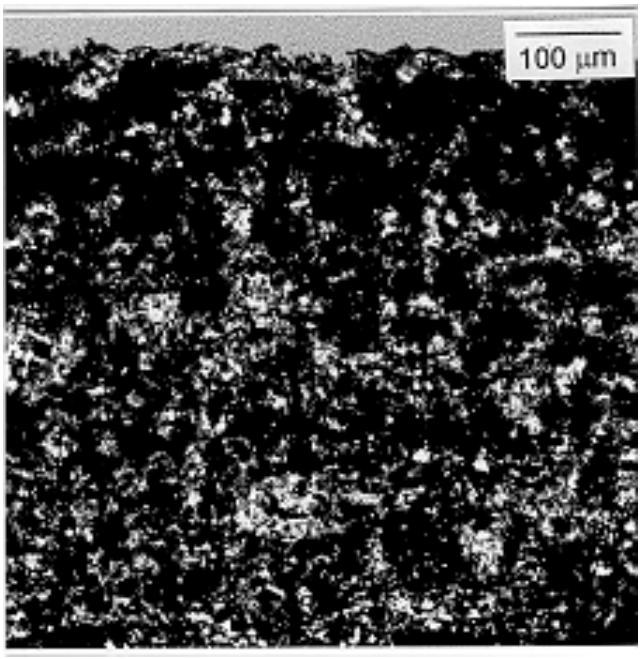

(a)

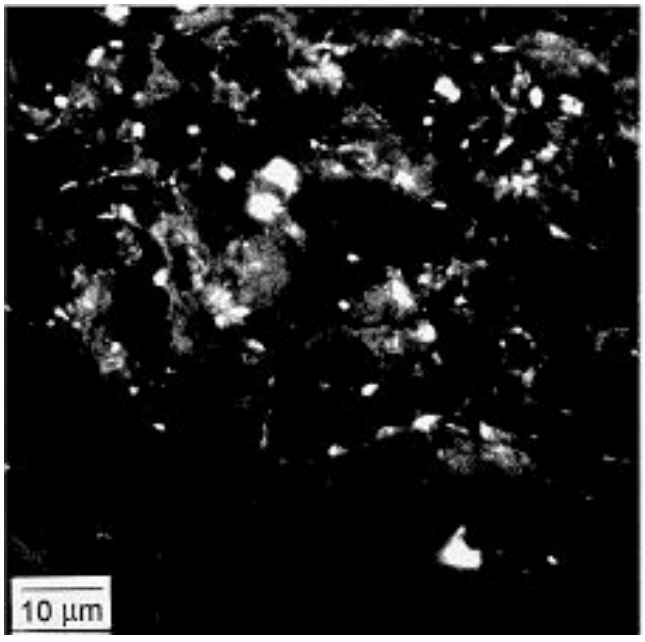

(b)

Fig. 3 (a) CLSM three-dimensional reconstruction of 12 *x-y* optical sections giving a volume of 500 by 500 by 21 μm^3. APS ceramic coating showing high density of defects. Impregnation from the free surface of the coating (top) reached the substrate/coating interface (dark bottom). (b) Detail of (a) CLSM three-dimensional reconstruction of 7 *x-y* optical sections showing the impregnation of a 61.4 by 61.4 by 6 μm^3 volume at the coating/substrate interface

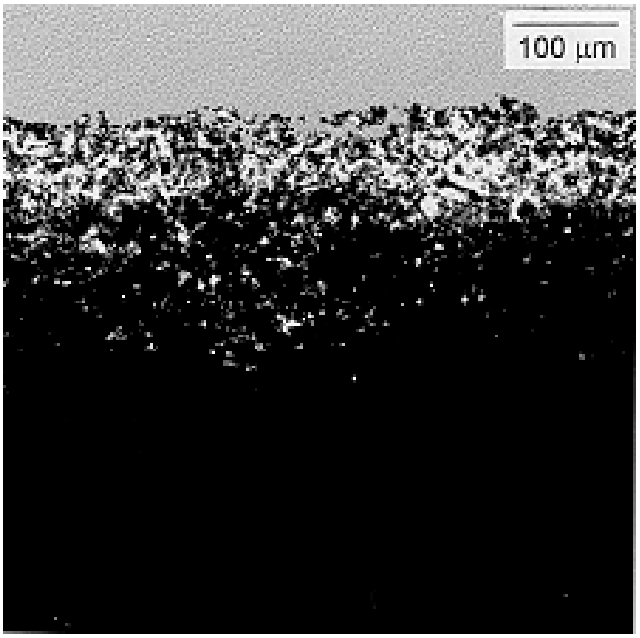

(a)

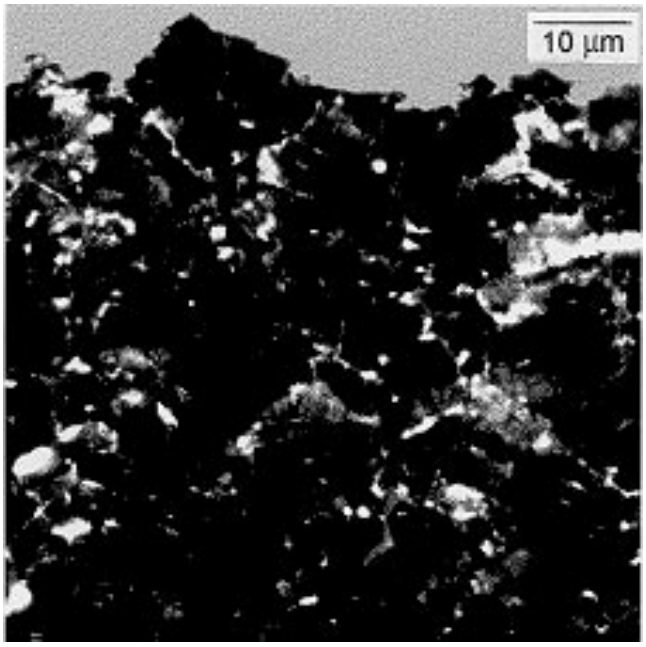

(b)

Fig. 4 (a) CLSM three-dimensional reconstruction of 16 *x-y* optical sections giving a volume of 500 by 500 by 16.5 μm^3. APS ceramic coating showing lower density of defects. (b) CLSM three-dimensional reconstruction of 7 *x-y* optical sections showing the impregnation in a 66.5 by 66.5 by 4.75 μm^3 volume. It is a detail from the top part of the coating.

The best results are obtained using a modified Spurr resin, its curing temperature being 60 °C, adding a compatible fluorescent dye to the resin and applying a vacuum of ~10^{-5} Pa. Also, the evacuation of the sample and the resin separately but simultaneously in these vacuum conditions impregnates fine and interconnected defects. Due to the characteristics of the fluorescent resin, they can be visualized with a CLSM. This allows additional information from the subsurface of the sample to be obtained without further preparation.

Defects generated during any necessary metallographic preparation would not contribute to the fluorescent image because the resin does not flow.

With the information obtained from the different optical sections, accurate quantitative image analysis can be carried out. The evolution of the defects in the *z*-axis can also be visualized from the CLSM images.

The proposed methodology has the advantage of being easy to perform, and, in addition, the resulting optical images give tridimensional information.

Relationships between defects (porosity or micro/macrocracking) and coating properties could be established more accurately applying the proposed methodology.

This method improves the quantification of the microcrack network connectivity.

Acknowledgment

The authors gratefully acknowledge Luc Bianchi and Nicolas Baradel, who kindly provided some of the samples for this study. Also, they would like to thank Mrs. Esther Vilalta and the Serveis cientific-tècnics of the University of Barcelona for their assistance.

References

1 J.P. Sauer, Testing and Characterization. The First Best Practice Challenge, *J. Therm. Spray Technol.*, Vol 4 (No.4), 1995, p 338-339

2. S.D. Glancy, Preserving the Microstructure of Thermal Spray Coatings, *Adv. Mater. Process.*, Vol 150, 1995, p 37-40
3. G.A. Blann, The Effects of Thermosetting and Castable Encapsulation Methods on the Metallographic Preparation of Ceramic Thermally Sprayed Coatings—A Technical Note, *J. Therm. Spray Technol.*, Vol 3 (No. 3), 1994, p 263-269
4. J.P. Sauer, The Effect of Mounting Process/Material on the Measured Porosity in Varied Thermal Spray Coatings, *United Thermal Spray Conference and Exposition* (UTSC'97) (Indianapolis, IN), 15-18 Sept 1997, ASM International, 1997
5. J.P. Sauer, The Recommended Practices Committee: Status of Metallurgical Preparation Procedure Format and the Round Robin (RR) for Determining Suggested Practices, *Thermal Spray: United Forum of Scientific and Technological Advances*, C.C. Berndt, Ed., ASM International, 1997, p 989
6. J. Karthikeyan, A.K. Sinha, and A.R. Biswas, Impregnation of Thermal Spray Coatings for Microstructural Studies, *J. Therm. Spray Technol.*, Vol 5 (No. 1), 1996, p 74-78
7. J.B. Pawley, Ed., *Handbook of Biological Confocal Microscopy*, Plenum Press, 1990
8. A.M. Glauert, Ed., *Practical Methods in Electron Microscopy*, Vol 3, North Holland/American Elsevier, 1974, p 136-138
9. N. Llorca-Isern, M. Español, and M. Puig, "Study of the Internal Defects of Coatings Using Confocal Microscopy," 12th Int. Conf. Surface Modification Technologies (Rosemont, IL), 12-15 Oct 1998
10. K. Murakami, C.-K. Lin, S.-H. Leigh, C.C. Berndt, S. Sampath, and H. Herman, et al., Porosity Measurement and Densification of Plasma Sprayed Alumina Titania Deposits, *Surface Modification Technologies XI*, T.S. Sudarshan, M. Jeandin, and K.A. Khor, Ed., The Institute of Materials, London, U.K., and ASM International, 1998, p 203-212
11. L. Bianchi, "Projection par Plasma d'arc et Plasma Inductif de Dépots Céramiques: Mécanismes de Formation de la Premiere Couche et Relation avec les Propriétés Mécaniques des Dépots," Ph.D. thesis, Université de Limoges, 1995 (in French)
12. N. Baradel, L. Bianchi, F. Blein, A. Freslon, and M. Jeandin, In situ Measurement within Plasma-Sprayed Zirconia Coatings under Industrial Conditions, *Proc. 15th Int. Thermal Spray Conf.*, C. Coddet, Ed., ASM International, 1998, p 563-574
13. H.J.G. Gundersen, T.F. Bendtsen, L. Korbo, N. Marcussen, A. Moller, K. Nielsen, J.R. Nyengard, B. Pakkenberg, F.B. Sorensen, A. Vesterby, and M.J. West, Some New, Simple and Efficient Stereological Methods and Their Use in Pathological Research and Diagnosis, *Acta Pathol., Microbiol. Immunol. Scand.*, Vol 96, 1988, p 379-394